Design, Testing, and Applications of Digital Microfluidics-Based Biochips

Krishnendu Chakrabarty
Department of Electrical and Computer Engineering
Duke University, Durham, NC 27708, USA
E-mail: krish@ee.duke.edu

Abstract

Microfluidics-based biochips offer a promising platform for massively parallel DNA analysis, automated drug discovery, and real-time biomolecular recognition. The first part of this paper introduces readers to digital microfluidics technology. The second part describes a recent technique for the automated design and synthesis of biochips. A clinical diagnostic procedure, namely multiplexed in-vitro diagnostics on human physiological fluids, is used to illustrate the design approach. The third part of the embedded tutorial is focused on test issues. It is important to ensure high reliability and availability of biochips as they are increasingly deployed for safety-critical applications. The tutorial includes a discussion of fault models, catastrophic fault testing, and concurrent test issues.

1. Introduction

Microfluidics-based biochips for biochemical analysis are receiving much attention nowadays [1]. These composite microsystems, also known as lab-on-a-chip or bio-MEMS, offer several advantages over conventional laboratory procedures. They automate highly repetitive laboratory tasks by replacing cumbersome equipment with miniaturized and integrated systems, and they enable the handling of small amounts, e.g., nanoliters, of fluids. Thus they are able to provide ultra-sensitive detection at significantly lower costs per assay than traditional methods, and in a significantly smaller amount of laboratory space.

An emerging application area for microfluidics is clinical diagnosis [2]. Microfluidics can also be used for countering bio-terrorism threats. Microfluidics-based systems, capable of continuous sampling and real-time testing of air/water samples for biochemical toxins and other dangerous pathogens, can serve as an always-on "bio-smoke alarm" for early warning.

Most microfluidic biochips of today contain permanently etched micropumps, microvalves, and microchannels, and their operation is based on the principle of continuous fluid flow [1]. A promising alternative is to manipulate liquids as discrete droplets [3]. Following the analogy of microelectronics, this novel approach is referred to as "digital microfluidics". Each droplet can be controlled independently and each cell in the array has the same structure. Therefore, in contrast to continuous-flow systems, droplet-based microfluidics offers reconfigurability as well as a scalable system architecture. These advantages make digital microfluidics-based biochips a promising platform for massively parallel DNA analysis, automated drug discovery, and real-time biomolecular detection.

As the use of digital microfluidics-based biochips increases, their complexity is expected to become significant due to the need for multiple and concurrent assays on the chip, as well as more sophisticated control for resource management. Time-to-market and fault tolerance are also expected to emerge as design considerations. As a result, current full-custom design techniques will not scale well for larger designs. There is a need to deliver the same level of CAD support to the biochip designer that the semiconductor industry now takes for granted. Moreover, it is expected that these microfluidic biochips are will be integrated with microelectronic components in next-generation system-on-chip designs. The 2003 International Technology Roadmap for Semiconductors (ITRS) clearly identifies the integration of electrochemical and electro-biological techniques as one of the system-level design challenges that will be faced beyond 2009, when feature sizes shrink below 50 nm [4].

Early research on CAD for digital microfluidics-based biochips has been focused on device-level physical modeling of single components [5]. While top-down system-level design tools are now commonplace in IC design, no such efforts have been reported for digital microfluidics chips. This embedded tutorial describes a system design and test methodology that attempts to apply classical synthesis techniques to the design of digital microfluidics-based biochips. This methodology speeds up the design cycle, reduce human effort, and increases dependability.

Figure 1 illustrates the design approach. A behavioral model for a biomedical assay is first manually obtained from the protocol for that assay. Next, architectural-level synthesis is used to generate a macroscopic structure of the biochip; this structure is analogous to a structural RTL model in electronic CAD. The macroscopic model provides an assignment of assay functions to biochip resources, as well as a mapping of assay functions to time-steps, based in part on the dependencies between them. Finally, geometry-level synthesis creates a physical representation at the geometrical level, i.e., the final layout of the biochip consisting of the configuration of the microfluidic array, locations of reservoirs and dispensing ports, and other geometric details.

The goal of a synthesis procedure is to select a design that minimizes a certain cost function under resource constraints. For example, architectural-level synthesis for microfluidics-based biochips can be viewed as the problem of scheduling assay functions and binding them to a given number of resources so as to maximize parallelism, thereby decreasing

Proceedings of the 18th International Conference on VLSI Design held jointly with 4th International Conference on Embedded Systems Design (VLSID'05)
1063-9667/05 $20.00 © 2005 IEEE

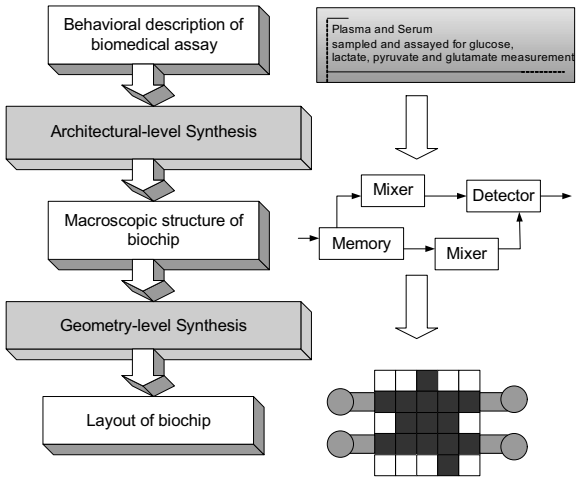

Figure 1. Synthesis methodology for digital microfluidics-based biochips.

response time. On the other hand, geometry-level synthesis addresses the placement of resources and the routing of droplets to satisfy objectives such as area, throughput or testability.

As droplet-based microfluidic systems are widely deployed in safety-critical biomedical applications, the reliability of these systems has emerged as a critical performance parameter. These systems need to be tested adequately not only after fabrication, but also continuously during in-field operation. For instance, for detectors monitoring for dangerous pathogens in critical locations such as airports, field testing is critical to ensure low false-positive and false-negative detection rates. In such cases, concurrent testing, which allows testing and normal biomedical assays to run simultaneously on a microfluidic system, can play an important role. It consequently facilitates built-in self-test (BIST) of microfluidic systems and makes them less dependent on costly manual maintenance on a regular basis.

Effective testing of biochips also requires an understanding of defects and realistic fault models. These fault models can serve as the basis of catastrophic and parametric fault testing, as well as tolerance analysis of microfluidic systems.

2. Review of State-of-the-Art

Synthesis of integrated circuits is a well-studied problem and advances in synthesis techniques continue even today. Driven by the need to integrate digital and analog functions in a mixed-signal circuit, analog circuit synthesis has gained momentum in recent years.

MEMS design is a relatively young field compared to IC design. Since the concept of special CAD systems for MEMS was first proposed at Transducer'87, several research groups have reported significant progress in this area, and a number of commercial MEMS CAD tools are now available [6, 7]. Many of these tools are focused solely on the modeling of thermal and mechanical properties. Recently, synthesis tools for MEMS have also been developed. However, because CAD tools for MEMS do not handle fluids, they cannot be directly used for the design of microfluidics-based biochips.

While MEMS design tools have reached a certain level of maturity, CAD tools for biochips are still in their infancy. For microfluidics-based biochips, some commercial computational fluid dynamics (CFD) tools, such as CFD-ACE+ from CFD Research Corporation and FlumeCAD from Coventor, Inc. support 3D simulation of fluidic transport. A recent release of CoventorWare from Coventor, Inc. includes microfluidic behavioral models to allow top-down system-level design. Unfortunately, this CAD tool is only able to deal with continuous flow systems and it is therefore inadequate for the design of digital microfluidics-based biochips.

Over the past decade, the focus in testing research has broadened from logic and memory test to include the testing of analog and mixed-signal circuits. MEMS is a relatively young field compared to IC design, and MEMS testing is still in its infancy. Recently, fault modeling and fault simulation in surface micromachined MEMS has received attention [8]. In [9], a comprehensive testing methodology for a class of MEMS known as surface micromachined sensors is presented.

However, test techniques for MEMS cannot be directly applied to microfluidic systems, since their actuation mechanism do not handle fluids. Most recent work in this area has been limited to the testing of continuous-flow microfluidic systems.

3. Digital Microfluidics-Based Biochips

The microfluidic biochip to be discussed in this tutorial is based on the manipulation of nanoliter droplets using the principle of electrowetting. Electrowetting refers to the modulation of the interfacial tension between a conductive fluid and a solid electrode by applying an electric field between them. The basic cell of a digital microfluidics-based biochip consists of two plates, and the filler medium, i.e., the silicone oil, sandwiched between the plates; shown in Figure 2. The droplets travel inside the filler medium. The bottom plate contains a patterned array of individually controllable electrodes, and the top plate is coated with a continuous ground electrode. The details of the fabrication process are described in [10]. By varying the electrical potential along a linear array of electrodes, droplets can be moved along this line of electrodes. The velocity of the droplet can be controlled by adjusting the control voltage (0~90V), and droplets can be moved at speeds of up to 20 cm/s. Based on this principle, microfluidic droplets can be moved freely to any location of a two-dimensional array without the need for micropumps and microvalves.

Using a two-dimensional array, many common operations for different biomedical assays can be performed, such as sample introduction (*dispense*), sample movement around the *transport*), temporarily sample preservation (*store*), and the mixing of different samples (*mix).* For instance, the *store* operation is performed by applying an insulating voltage droplet. The *mix* operation is used to route two droplets to the same location and then turn them around some pivot points.

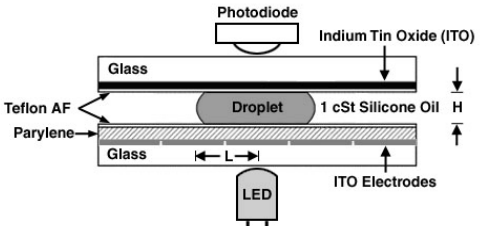

Figure 2. Digital microfluidics-based biochip used in colorimetric enzymatic assay.

The configurations of the microfluidic array, i.e., the routes that droplets travel and the rendezvous points of droplets, are programmed into a microcontroller that controls the voltages of electrodes in the array. In this sense, thee mixers and storage units in the array can be viewed as reconfigurable virtual devices.

3.1. Application: Multiplexed *in-vitro* Diagnostics on Human Physiological Fluids

The *in-vitro* measurement of glucose and other metabolites, such as lactate, glutamate and pyruvate, in human physiological fluids is of great importance in clinical diagnosis of metabolic disorders. For instance, the change of regular metabolic parameters in the patient's blood can signal organ damage or dysfunction prior to observable microscopic cellular damages or other symptoms. The feasibility of performing a colorimetric enzyme-kinetic glucose assay on a digital microfluidics-based biochip has been successfully demonstrated in experiments [11]. This full-custom biochip consists of a basic microfluidic platform, which moves and mixes droplets containing biomedical samples and reagents, several reservoirs that store and generate the droplets of samples and reagents, and an integrated optical detection system consisting of a LED and a photodiode; see Figure 1.

In addition to glucose assays, the detections of other metabolites such as lactate, glutamate and pyruvate in a digital microfluidics-based biochip have also been demonstrated recently [11]. Using similar enzymatic reactions and modified reagents, these assays as well as the glucose assay can be integrated to form a multiplexed *in-vitro* diagnostics on different human physiological fluids, which can be performed concurrently on a microfluidic biochip.

5. Architectural Synthesis

In this section, we focus on the problem of scheduling bioassay operations under resource constraints. An example of a real-life biochemical procedure is used to evaluate the proposed methodology. Since the scheduling problem is NP-complete, heuristics are used to solve the problem in a computationally efficient manner. Experiments show that for a representative set of bioassays, the results obtained from the heuristics are close to provable lower bounds.

5.1 Sequencing Graph Model

The behavioral description of an example of multiplexed *in-vitro* diagnostics is shown in Figure 2. Four types of human physiological fluids—plasma, serum, urine and salvia—are

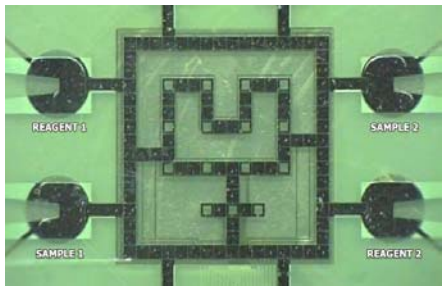

Figure 3. Fabricated microfluidic array used for multiplexed biomedical assays.

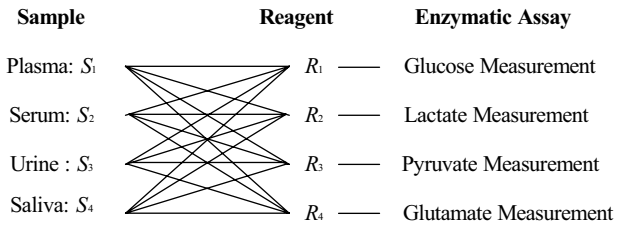

Figure 4. One example of multiplexed *in-vitro* diagnostics.

sampled and dispensed into the microfluidic biochip. Next each type of physiological fluid is assayed for glucose, lactate, pyruvate or glutamate measurement. The result of the biomedical assay is detected by an integrated optical absorbance measurement device.

An abstract model of a biomedical assay behavior at the architectural level can be developed in terms of operations and the dependencies between them [12]. We use the sequencing graph model from high-level synthesis. We assume that there are a total of n_{ops} operations. The sequencing graph is acyclic and polar. There are two vertices, called source v_0 and sink v_k, that present the first and last no-operation task, where $k = n_{ops} + 1$. Hence the sequencing graph $G(V, E)$ has vertex set $V = \{v_i: i = 0, 1,\ldots, k\}$ in one-to-one correspondence with the set of assay operations, and edge set $E = \{(v_i, v_j): i, j = 0, 1,\ldots, k\}$ representing dependencies. With each node v_i, we associate a weight $d(v_i)$, which denotes the time taken for operation v_i. The details of these operations and the resources that these operations use are as follows. (We assume that m types of physiological fluids are assayed for n types of enzymatic measurements.)

1. Input Operations: These operations consists of the generation of the droplets of samples (S_i, i =1,…, m) or reagents (R_i, i =1,…, n) from the on-chip reservoir, which are then dispensed into the microfluidic array. There are $m+n$ types of input operations (denoted by I_i, i =1,…, $m+n$), where I_j, j =1,…, m represents the generation and dispensing of droplets of sample S_j. Similarly, I_{j+m}, j=1,…, n, denotes the operation for reagent R_j.

In order to avoid unexpected contamination between different samples and reagents, at least one reservoir is needed for each type of fluid. We assume that there are Nr reservoirs for each type of fluid ($Nr \geq 1$). Moreover, these

reservoirs belong to the category of non-reconfigurable resources, i.e., they are fixed after design and fabrication.

2. Mixing operation: In order to perform the required enzymatic assay, droplets of samples need to be mixed with droplets of reagents on the microfluidic array. We define m types of mixing operations $M_1, \ldots, M_m$.

The weights of the nodes, i.e., mixing times, representing the different type of mixing operations are different; for example, $d(M_1) = 5$ for plasma, $d(M_2) = 3$ for serum, $d(M_3) = 4$ for urine, and $d(M_4) = 6$ for saliva. The resources corresponding to these mixing operations are reconfigurable mixers.

3. Detection operation: After mixing, the results of biomedical assay are detected using an integrated LED-photodiode setup. The weights of the nodes representing different type of detection are different. For an instance, $d(D_1) = 5$ for glucose, $d(D_2) = 4$ for lactate, $d(D_3) = 6$ for pyruvate, and $d(D_4) = 5$ for glutamate measurements. The resources corresponding to these operations are integrated optical detectors consisting of a LED-photodiode setup. At least one detector is needed for each type of enzymatic assay. We assume that there are Nd detectors for each type of assay ($Nd \geq 1$). These resources also belong to the category of non-reconfigurable resources.

After defining all the basic operations, the multiplexed in-vitro diagnostics on human physiological fluids can now be modeled by the sequencing graph shown in Figure 6.

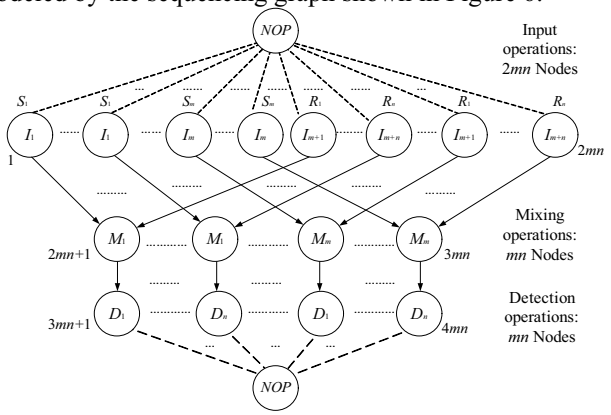

Figure 5. Sequencing graph model of a multiplexed biomedical assay.

It is important to note that for optimal scheduling of assay operations under resource constraints, the memory resource also needs to be considered. If two sequential operations are not scheduled in consecutive time-steps, the storage unit, i.e., memory resource, is required to store the droplet temporarily. These memory resources are also reconfigurable. In addition, the number of storage units is inversely proportional to the number of available mixers because the total number of cells in the array is fixed. This constraint adds to the complexity of the scheduling problem. A mathematical programming model for the scheduling problem is described in [12].

5.2. Heuristics for the Scheduling Problem

The scheduling problem being studied here is equivalent to the resource-constrained scheduling problem with non-uniform weights of operation nodes, which has been proven to be NP-complete. In order to solve this problem in a computationally efficient manner, two heuristics are described in [12].

Modified *List Scheduling* Algorithm (M-LS). This heuristic extends the well-known *List Scheduling* algorithm to handle reconfigurable resources such as mixers and storage units. Operations are sorted in topological orders based on the dependency constraints. In each time step, operations are evaluated and then the ready ones are found. If the number of ready operations of a single type exceeds the number of the available resources to cover them, then some operations must be deferred. The selection procedure is determined by a defined priority list of the operations.

Heuristic Based on a Genetic Algorithm (GA). A robust representation technique called *random keys* is used for chromosome representation. Each chromosome in the population can be encoded as a vector of random keys. In other words, *Chromosome* = {*gene*(*1*)*,…, gene*(*k*)*, gene*(*k*+1)*,…, gene*(2*k*)}, where k is the number of operations. Each gene is a random number sampled from [0, 1]. The first k genes are used to indicate the operation priorities, i.e., priority value of operation $Pv(i) = gene(i)$, i = 1 to k. The last k genes are used to determine the delay time of the operations, which is calculated as follows: delay value of operation $Dv(i) = d \times MaxDur \times gene(i+k)$, $i = 1$ *to* k, where d is a constant. These delay values are further modified in the schedule construction procedure, such that any random number ($gene(i+k)$) can be used to form the feasible solution.

An *ad-hoc* procedure is used to construct a feasible schedule, i.e., satisfying dependency and resource constraints, by using a vector of random numbers (chromosome). It consists of three phases: scheduling input operations, scheduling for mixing operations and scheduling optical detection operations. Using these three phases, a feasible schedule satisfying both dependency constraints and resource constraints can be constructed using any random key vector.

In a genetic algorithm, reproduction and crossover operators tend to increase the quality of the populations and force convergence, while mutation opposes convergence and replaces genes lost during reproduction and crossover. In the heuristic approach of [12], these evolutionary operators are defined as follows:

Reproduction: The chromosomes that have the highest fitness value, i.e., the smallest completion time of the generated schedule, in the current population are copied to the next generation.

Crossover: Parameterized uniform crossover is employed in [12]. In this crossover procedure, two parent chromosomes are chosen randomly from the old population. Then gene(i) of their offspring in the new population is inherited (i.e., copied) from gene(i) of the father chromosome with the probability P (e.g., 0.7), and from the mother chromosome with the probability $1-P$.

Mutation: The new chromosomes of the population are generated randomly to guarantee population diversity.

5.3. Simulation Experiments

Five real-life examples have been used in [12] to evaluate the heuristics. The details are presented in Table 1.

Table 1. Five example experiments (S_1: Plasma, S_2: Serum, S_3: Urine, S_4: Saliva, Assay1: Glucose assay, Assay2: Lactate assay, Assay3: Pyruvate assay, Assay4: Glutamate assay**).**

Example	Description	Node weights for mix operations	Node weights for detection operations
Example 1 (Nr=Nd=1 Na=3) m=2, n=2	S_1 and S_2 are assayed for Assay1 and Assay2.	$d(M_1)$ = 5 for S_1 $d(M_2)$ = 3 for S_2	$d(D_1)$=5 for Assay1 $d(D_2)$=4 for Assay2
Example 2 (Nr=Nd=1 Na=4) m=2, n=3	S_1, and S_2 are assayed for Assay1, Assay2, and Assay3.	$d(M_1)$ = 5 for S_1 $d(M_2)$ = 3 for S_2	$d(D_1)$=5 for Assay1 $d(D_2)$=4 for Assay2 $d(D_3)$=6 for Assay3
Example 3 (Nr=Nd=1 Na=5) m=3, n=3	S_1, S_2, and S_3 are assayed for Assay1, Assay2, and Assay3.	$d(M_1)$ = 5 for S_1 $d(M_2)$ = 3 for S_2 $d(M_3)$ = 4 for S_3	$d(D_1)$=5 for Assay1 $d(D_2)$=4 for Assay2 $d(D_3)$=6 for Assay3;
Example 4 (Nr=Nd=1 Na=7) m=3, n=4	S_1, S_2, and S_3 are assayed for Assay1, Assay2, Assay3 and Assay4.	$d(M_1)$ = 5 for S_1 $d(M_2)$ = 3 for S_2 $d(M_3)$ = 4 for S_3	$d(D_1)$=5 for Assay1 $d(D_2)$=4 for Assay2 $d(D_3)$=6 for Assay3 d(D$_4$)=5 for Assay4
Example 5 (Nr=Nd=1 Na=9) m=4, n=4	S_1, S_2, S_3 and S_4 are assayed for Assay1, Assay2, Assay3 and Assay4.	$d(M_1)$ = 5 for S_1 $d(M_2)$ = 3 for S_2 $d(M_3)$ = 4 for S_3 $d(M_4)$ = 6 for S_4	$d(D_1)$=5 for Assay1 $d(D_2)$=4 for Assay2 $d(D_3)$=6 for Assay3 d(D$_4$)=5 for Assay4

The modified *list scheduling* algorithm (M-LS) and *genetic algorithm*-based heuristic (GA) are applied to these five examples. The simulation results are shown in the Table 2. For the smaller problem instances corresponding to Example 1 and Example 2, the optimal solutions have been obtained using the ILP model. (For the other three problem instances, the ILP model did not yield a solution within reasonable time.) Upper bounds and lower bounds are also listed in the Table 2.

The results show that both M-LS and GA are able to generate good solutions, which are very close to the lower bounds. The ratio of the completion time obtained using the heuristic methods to the lower bound is no more than 1.2 in most cases. While GA yields lower completion times than M-LS, it has O(n^2) complexity compared to the O(n) complexity for M-LS, where n is the number of operations.

Table 2. Completion time (in time units; 1 time unit = 2 seconds**).**

Experiment	Opt	LB	UB	M-LS	GA
Example 1	15	15	23	17	15
Example 2	17	17	25	19	17
Example 3	N/A	23	47	26	25
Example 4	N/A	23	43	27	26
Example 5	N/A	29	59	35	34

6. Testing of Digital Biochips

Faults in digital microfluidic systems can be classified as being either catastrophic or parametric. Catastrophic (hard) faults lead to a complete malfunction of the system, while parametric (soft) faults cause a deviation in the system performance. A parametric fault is detectable only if this deviation exceeds the tolerance in system performance.

Catastrophic faults may be caused by the following physical defects:

- *Dielectric breakdown*: The breakdown of the dielectric at high voltage levels creates a short between the droplet and the electrode. As a result, no charge can be stored in the interface. As the electrowetting mechanism depends on the amount of energy stored in the capacitor formed by the electrode and the droplet, dielectric breakdown inhibits fluid motion.
- *Short between the adjacent electrodes*: As a result of a short circuit between two adjacent electrodes, these electrodes effectively form one longer electrode. Thus, the droplet residing on this electrode is no longer large enough to overlap with the adjacent electrodes, inhibiting its actuation.
- *Degradation of the electrode:* This degradation effect is unpredictable and may become catastrophic during the operation of the system. A consequence of electrode degradation is that droplets often fragment and their motion is prevented because of the unwanted variation of surface tension forces along their flow path.
- *Open in the metal connection between the electrode and the control source*: This defect results in a failure of charging electrode while trying to drive the droplet.

Physical defects that cause parametric faults include the following:

- *Geometrical parameter deviation:* The deviation in insulator thickness, electrode length, and height between parallel plates may exceed their tolerance value.
- *Insulator degradation:* This "wear-and-tear" defect may become apparent gradually during operation. If left undetected, it may eventually cause electrode degradation.
- *Particle contamination:* During in-field operation of a microfluidic system, the droplet or the filer fluid may be contaminated by a particle, such as a dust particle or a foreign fluid droplet. Typically such particles are then attached to the surface of the insulator of a cell and affect the motion of the droplet.
- *Change in viscosity of droplet and filler medium.* These deviations can occur during the operation due to an unexpected biochemical reaction, or a defect in the control system causing unwanted temperature variation.

Faults in microfluidic systems can also be classified based on the time at which they appear. Therefore, system failure or degraded performance can either be caused by manufacturing defects or by parametric variations. Testing of manufacturing defects, such as a short between the adjacent electrodes or a deviation in the value of the geometrical parameters, should be performed immediately after production. However, operational faults, such as degradation of the insulator or change in fluid viscosity, can occur throughout the lifetime of the system. Therefore, concurrent

testing during system operation is essential to ensure the operational health of safety-critical systems.

In the testing methodology discussed in [13], test droplets (e.g., 0.1M KCL) are released into the microfluidic system from droplet sources and are guided through the system following the designed testing scheme. Both catastrophic and parametric faults are detected by electrostatically controlling and tracking the motion of these test stimuli droplets. This testing method is minimally invasive and easy to implement, which offers an opportunity to eradicate the need for expensive and bulky external devices.

To facilitate a decision-making process, a detection mechanism is needed for both catastrophic and parametric faults. This mechanism needs to be based on a pass/fail criterion that yields the some response to each of the possible faults to prevent masking among various types of faults. The unified detection mechanism in [13] consists of a simple RC oscillator circuit formed by the sink electrodes and the fluid between them as an insulator; see Figure 4. The capacitance of this structure depends on the presence of the droplet since the filler medium and the droplet have distinct permittivity values. By sensing the capacitance of this structure through a simple frequency counter, one can determine whether a droplet has reached the sink. This mechanism can be electronically implemented and easily integrated on-chip. In order to provide a unidirectional and unambiguous detection mechanism, the pass/fail criterion has to be determined based on the presence of the droplet at the sink electrode and this criterion should be applied for all test cases. Fault-free operation is associated with the presence of the droplet at the sink electrode and faulty operation with its absence.

This cost-effective fault testing procedure can be performed simultaneously with a normal bioassay on a microfluidic system [14]. Such a concurrent testing methodology can be used for field-testing of droplet-based microfluidic systems; as a result, it increases the system reliability during everyday operation. With negligible hardware overhead, this method also offers an opportunity to implement BIST for microfluidic systems and therefore eliminates the need for costly, bulky, and expensive external test equipment. Furthermore, after detection, droplet flow paths for biomedical assays can be reconfigured dynamically such that faulty cells are bypassed without interrupting the normal operation. Thus, this approach increases fault-tolerance and system lifetime when such systems are deployed for safety-critical applications.

6. Conclusions

We have presented an overview of droplet-based microfluidic systems and shown how to apply classical architectural-level synthesis can be used to design microfluidics-based biochips. A clinical diagnostic procedure, namely multiplexed *in-vitro* diagnostics on human physiological fluids, has been used to illustrate this methodology. We have also presented a classification of faults in such systems, and discussed how they can be detected. These techniques are therefore expected to pave the way for the deployment of reliable bio-MEMS and lab-on-a-chip devices for safety-critical applications.

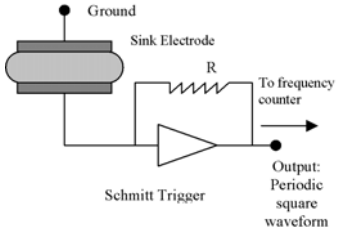

Figure 6. Unified fault detection mechanism.

Acknowledgements

The author thanks Fei Su for contributing to this paper. This work is supported by the National Science Foundation under grant no. EIA-0312352.

References

[1] E. Verpoorte and N. F. De Rooij, "Microfluidics meets MEMS", *Proc. IEEE*, vol. 91, pp. 930 - 953, 2003.

[2] C.H. Ahn et al., "Disposable smart lab on a chip for point-of-care clinical diagnostics", *Proc. IEEE*, vol. 92, pp.154-173, 2004.

[3] M.G. Pollack, R.B. Fair and A.D. Shenderov, "Electrowetting-based actuation of liquid droplets for microfluidic applications", *Applied Physics Letters*, vol. 77, pp. 1725-1726, 2000.

[4] International Technology Roadmap for Semiconductor (ITRS), http://public.itrs.net/Files/2003ITRS/Home2003.htm.

[5] B. Shapiro et al., "Modeling of electrowetted surface tension for addressable microfluidic systems: dominant physical effects, material dependences, and limiting phenomena" *Proc. IEEE Conf. MEMS*, pp. 201- 205, 2003.

[6] G. K. Fedder and Q. Jing, "A hierarchical circuit-level design methodology for microelectromechanical system", *IEEE Trans. Circuits and Systems II,* vol. 46, pp.1309-1315, 1999.

[7] S. K. De and N. R Aluru, "Physical and reduced-order dynamic analysis of MEMS", *Proc. IEEE/ACM IC-CAD*, pp. 270-273, 2003.

[8] S. Mir, B. Charlot and B. Courtois. "Extending fault-based testing to microelectromechanical systems." *Journal of Electronic Testing: Theory and Applications,* vol. 16, pp. 279-288, 2000.

[9] N. Deb and R. D. Blanton, "Analysis of failure sources in surface-micromachined MEMS", *Proc. IEEE Int. Test Conf.*, pp. 739-749, 2000.

[10] M. G. Pollack, A. D. Shenderov and R. B. Fair, "Electrowetting-based actuation of droplets for integrated microfluidics", *Lab on a Chip*, vol. 2, pp. 96-101, 2002.

[11] V. Srinivasan, V. K. Pamula, M. G. Pollack and R. B. Fair, "A digital microfluidic biosensor for multianalyte detection", *Proc. IEEE Conf. MEMS*, pp. 327-330, 2003.

[12] F. Su and K. Chakrabarty, "Architectural-level synthesis of digital microfluidics-based biochips", accepted for publication in *Proc. IEEE Int. Conf. CAD*, 2004.

[13] F. Su, S. Ozev and K. Chakrabarty, "Testing of droplet-based microelectrofluidic systems", *Proc. IEEE International Test Conference*, pp. 1192-1200, 2003.

[14] F. Su, S. Ozev and K. Chakrabarty, "Concurrent testing of droplet-based microfluidic systems for multiplexed biomedical assays", accepted for publication in *Proc. International Test Conference*, 2004.